Neutron Count Rate Calculation in GADRAS Version 15.3

Dean J. Mitchell, Lee T. Harding, John K. Mattingly, and James L. Barnett
Contraband Detection Department 6418

July 7, 2009

Sandia National Laboratories
P.O. Box 5800
Albuquerque, New Mexico 87185-0782

SAND 2009-4321P

Abstract

This document describes the neutron detector response function and the neutron interface in GADRAS Version 15.3. Data are presented to compare computed neutron count rates with measurements as a function of the distance and height for selected detectors. This software version represents a substantial improvement in the accuracy of neutron calculations relative to previous versions. An observation that was made in the course of this study is that reflected neutrons may account for more than 90% of the counts recorded by minimally-moderated ^{3}He detectors, and an inverse distance-squared relationship is a very poor representation of how counts vary with distance.

1. Introduction

The Gamma Detector Response and Analysis Software (GADRAS) incorporates an empirical response function for neutron detectors. Once a detector has been characterized, neutron count rates can be used to confirm analyses results, or the neutron measurements can be applied along with gamma-ray measurements to determine masses of nuclear materials. The neutron detector response function has been modified recently to more quantitatively characterize neutrons that impact the detector after reflection from the floor and/or ceiling. Although the fact that reflection can alter neutron count rates has always been recognized, characterization of how this alters the count rate has been neglected in software that was released before 2008 because neutron reflection is a secondary consideration for well-moderated detectors that are characterized at distances and heights that are similar to conditions under which the instruments will be used. A new challenge that has arisen in recent years is that hand-held instruments with minimally moderated ^{3}He tubes (or other thermal-neutron detectors) are now widely used to perform inspections for concealed nuclear materials. It is not possible to know in advance how inspectors will use the instruments, so analysts must be able to accommodate a variety of conditions. Computed neutron count rates must also be accurate in order to evaluate the performance of existing sensors or proposed detector concepts.

2. Neutron Detector Response Function

2.1 Interpolation of Monte Carlo Calculations

A detector response function was developed in 1993 for neutrons to simplify a detector characterization procedure using semi-empirical techniques [1]. This response function was based on interpolation among a series of pre-computed detector efficiency curves for an array of ^{3}He tubes with various thicknesses of polyethylene surrounding both the front and the back of the tubes. The neutron efficiency curves were computed with the general purpose Monte Carlo transport code MCNP (Monte Carlo N-particle) [2]. The original formulation of the neutron response function utilized the following parameters:

- moderator area
- thickness of polyethylene on the front of the detector
- thickness of polyethylene on the back of the detector
- percent of the surface that is covered with cadmium (to absorb thermal neutrons)
- an efficiency scalar

The first four parameters are known from the detector design and can be asserted to fit based on measurements of a ^{252}Cf source in various moderator thicknesses, which produces a range of neutron energy profiles. The efficiency scalar is an empirical parameter that combined effects associated with differences in the ^{3}He pressure, the spacing between the tubes, and environmental effects. Even though the response of a ^{3}He detector was used as a basis for the Monte Carlo calculations that are used as a basis for the model, the response function would also apply to other types of thermal neutron detectors with appropriate adjustment of the empirical efficiency scalar. According to this simple neutron detector model, the count rate for a detector is computed according to the following relationship:

$$R = \Omega \sum_{j=1}^{n} \dot{N}_j \varepsilon_j \qquad (1)$$

where Ω is the solid angle, n is the number of energy groups for the neutron leakage, $\dot{N}_j$ is the neutron leakage rate in energy group j (neutrons/second). The gross detector efficiency for energy group j is given by ε_j, which is defined as the gross number of counts per neutron that directly impacts the front surface of the detector. The rate at which neutrons impact the front surface of the detector without reflection from materials in the vicinity of the detector is given by the total neutron emission rate times the solid angle, which is given by Eq. (2):

$$\Omega = 0.5 \left(1 - \frac{1}{\sqrt{1 + \left(\frac{r}{d} \right)^2}} \right) \qquad (2)$$

where r is the radius of a circular detector with the same cross-sectional area as the actual detector, and d is the distance from the source to the front surface of the detector.

The methodology that was developed in the original neutron detector response model was extended in a recent development that improves the accuracy of the neutron detector response. [3] The principal factor that resulted in improved accuracy is the use of a new neutron energy group structure (Kynea3), which uses fine energy bins in the thermal region. The Kynea3 energy group structure enables computation of neutron up-scattering and generally provides a more accurate representation of the neutron profile for well-moderated sources.

The revised neutron detector response model explicitly differentiates neutrons that impact the detector directly from neutrons that strike the detector after reflection from the ground and ceiling materials. As shown in Eq. (3), the gross efficiency parameter has been replaced by the parameters $\omega_{j,k}$, which define the efficiencies in energy groups j for the front, back, and sides of the detector, respectively. These efficiency parameters define the net counts recorded per neutron that strikes each of the detector surfaces. The contribution of the reflected neutrons is represented by the second term in Eq. (3). The parameters A_k represent the surface areas for the front (k=1), back (k=2), and sides (k=3) of the detector. Elements of a computed reflection matrix are given by $M_{i,j}$, which represents the neutron flux in energy group i per neutron that is emitted by the source in energy group j. The reflection matrix gives the average flux (neutrons/s) into a volume element at the distance and height of the detector. In general, the flux will not be the same on all surfaces, and differences in the angular distribution of the flux values are represented by ratios of the flux into the front (J_1), back (J_2), and sides of the detector (J_3) relative to the

average flux, $\bar{J}$. Calculations that were used to define the reflection matrix assume that the source is located at the same elevation as the center of the detector.

$$R = \sum_{j=1}^{n} \dot{N}_j \left[\Omega \omega_{j,1} + \sum_{i=1}^{n} M_{i,j} \sum_{k=1}^{3} \left(\frac{J_k}{\bar{J}} \right) A_k \omega_{i,k} \right] \quad (3)$$

Count rates given by Equations (1) and (3) can be equated to derive the relationship between the gross count rate, ε_j, and the terms from Eq. (3). The count rate associated with neutrons emitted in each of the source energy groups is independent of neutrons emitted in other energy groups, so the values are identical for each of the terms within the source energy group summation (i.e., index j). Therefore, the gross efficiency for source energy group j is given by the following relationship:

$$\varepsilon_j = \omega_{j,1} + \frac{\sum_{i=1}^{n} M_{i,j} \sum_{k=1}^{3} \left(\frac{J_k}{\bar{J}} \right) A_k \omega_{i,k}}{\Omega} \quad (4)$$

The flux of reflected neutrons is computed by interpolating a table that was computed using NCMP5. The table defines the energy spectrum of reflected neutrons as a function of the source neutron energy and the environment. The table includes entries for the following environments:

1. outside of buildings or in a large bay
2. within a building, above a suspended floor
3. within a building, above a concrete floor directly on the ground

In each of these environments, the source and detector are assumed to be located at the same distance above the ground. The first environment only includes the presence of a 6”-thick concrete slab poured directly on the ground. The second environment includes a 4”-thick concrete floor and a 4”-thick concrete ceiling at a height of 10 feet. The third environment includes a 6”-thick concrete slab poured directly on the ground and a 4”-thick concrete ceiling at a height of 10 feet.

2.2 Neutron Reflection Model

GADRAS computes the flux of reflected neutrons on the detector surfaces by interpolating tables that were computed using MCNP5 [2, 4]. The models that were used to compute the flux tables included only a floor or a floor and a ceiling. The simple models do not fully describe all of the interactions between the neutrons and the environment, and empirical corrections were required to accurately reproduce measurements. The empirical scale factors were established to replicate the response of the bare ^{3}He tube and the ^{3}He tube with the 1”-thick polyethylene moderator within a typical laboratory. The distances ranged from 50 cm to 200 cm and heights ranged from 50 cm to 150 cm. This environment is described as “Indoors above suspended floor” in the GADRAS interface. The same scale factors are applied to the other two environments that are supported by GADRAS. The scale factors are not accessible to general users, who only need to define a few parameters that are directly related to the detector design, such as the moderator area and moderator thicknesses. The application provides support for fitting these parameters empirically. Alternatively, the GADRAS installation also creates folders for common types of neutron detectors, and the associated response parameters can be applied directly without additional characterization (see Section 5).

3. Experimental Procedure

Measurements of neutron count rates were performed using several detectors and neutron source configurations for a series of distances ranging from 50 to 200 cm and heights ranging from 50 cm to 150 cm. Measurements were performed near the center of a laboratory that is approximately 8 meters long by 5 meters wide. Except for benches and small pieces of equipment that lined the exterior of the laboratory, no other materials were present during measurements and personnel stayed as far as

reasonably possible from the source and detector. The following neutron detectors were used to perform these measurements:

- 13”-long (12” active length), 1”-diameter, 10-atmosphere ^{3}He tube with no moderator
- 13”-long (12” active length), 1”-diameter, 10-atmosphere ^{3}He tube inserted into a 1”-thick polyethylene sleeve
- Ortec Detective-EX-100
- Exploranium GR-135 (neutrons are detected with a LiI solid-state detector)

Distances were measured from the center of the neutron source to the centerline of the ^{3}He tube in the first two detector configurations, and the axis of the ^{3}He tube was horizontal and perpendicular to the source. Distances were measured from the center of the neutron source to the front faces of the Detective-EX-100 and the GR-135. The radiation source and the center of the neutron detector were always placed at the same height relative to the floor. Figure 1 shows a representative source and detector arrangement during one of the neutron count rate measurements.

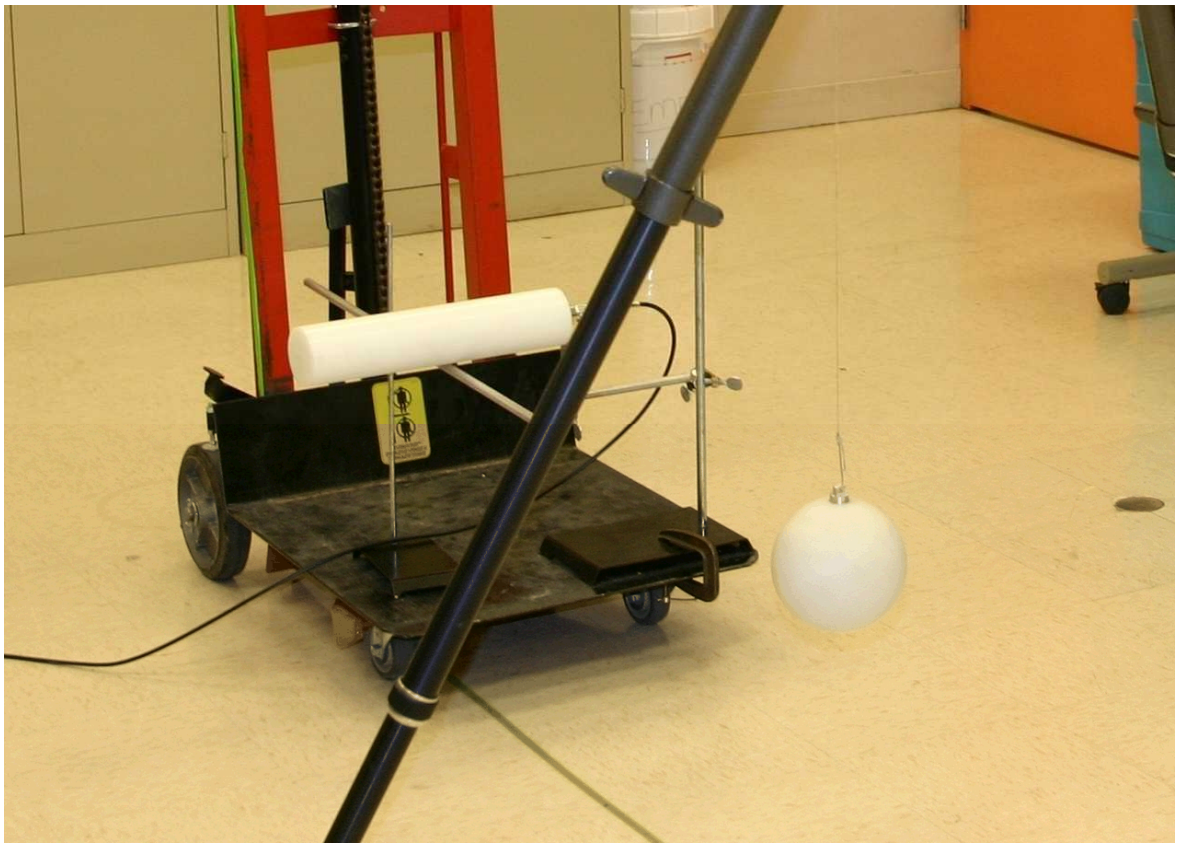

Fig. 1. Source and detector arrangement during a neutron count-rate measurement. The ^{3}He tube inside the 1″-thick polyethylene moderator is the horizontal cylinder supported by the hand truck and the ^{252}Cf source is inside the spherical moderator in the foreground.

The neutron source set consisted of a ^{252}Cf source that was measured bare and in a series of polyethylene spheres that produced a range of neutron energy profiles. The moderators ranged from 1 to 8 centimeters thick. The configurations also included borated polyethylene moderators, which altered the neutron-energy profile by eliminating most of the neutrons in the thermal region while retaining the epithermal neutrons.

4. Results

Measurements described in Section 3 were used to establish empirical scale parameters based on the performance of the bare ^{3}He tube and the ^{3}He tube within the 1”-thick cylindrical moderator. Although it was not possible to obtain perfect agreement over the large range of distances, heights, and moderator thicknesses that were included in the measurements series, computed neutron count rates generally agree with measurements within 10% for these detector configurations. Similar series of measurements were also performed with a Detective-EX-100 and a GR-135 in order to evaluate the ability of the response model to predict the performance of detectors that were not used to establish the empirical parameters. The commercial detectors also represent detector configurations that are less amenable to simple, idealized descriptions.

If not for reflected neutrons, the neutron detection efficiency for a given source would be constant if the efficiency is defined as the counts per neutron that strike the detector without any environmental interactions. In fact, the response model that was contained in GADRAS prior to the release of Version 14.8 in October 2008 did not account for reflected neutrons, so the predicted efficiency was independent of both distance and height. Consequently, computed neutron count rates were only accurate if distance and height for the characterization measurements were approximately the same as the configuration for the measurement that was to be analyzed. In order to provide generalized applicability, the response function must incorporate a characterization of reflection neutrons. This is particularly important for minimally moderated detectors such as those in most handheld sensors. The bare ^{3}He tube represents an extreme case because it has almost no sensitivity to the high-energy neutrons that are emitted directly by the unmoderated ^{252}Cf source. Figure 2 compares measured and computed neutron detection efficiencies for the bare ^{3}He tube when it was exposed to an unmoderated ^{252}Cf source. In this case, the detector efficiency increases by more than a factor of ten as the source-to-detector distance changes from 50 to 200 cm. The average efficiency is about 100 times greater than the efficiency that would have been observed in the absence of reflected neutrons. The detection efficiency is less affected by neutron reflection for moderated sources or moderated neutron detectors. The reduced influence of reflected neutrons is illustrated in Fig. 3, which compares measured and computed neutron detector efficiencies for the ^{3}He tube inside a 1”-thick polyethylene moderator. Even though the dependence on distance is reduced, the efficiency still varies by almost a factor of three over this range of distances. The detection elements in most handheld detectors are surrounded by less than 1 inch of moderator, so the variability of the efficiency falls somewhere in between the characteristics of the bare ^{3}He tube and the ^{3}He tube within the 1”-thick moderator.

Figures 4 through 11 show the correlations between measured net (background subtracted) count rates and computed neutron count rates for the four detectors that were included in the series of neutron measurements that are described in this document. Figure 4 is an interesting case because this plot shows that the count rate has very little dependence on distance when an unmoderated ^{3}He tube is used to measure the count rate associated with an unmoderated ^{252}Cf source. The degree of correlation between measured and computed count rates for the Detective-EX-100 and the GR-135 is about as good as the performance of the bare and moderated ^{3}He tube. Since the commercial detectors were not included in the evaluation of empirical parameters as described in Section 2.2, this observation suggests that the characterization of reflected neutrons also appears to apply to other types of detectors. The detector model, which is based on the response of a ^{3}He detector, also applies well to the Li scintillator in the GR-135. Although the principal objective of the measurements that are reported here was to validate the neutron count-rate calculations, measurements recorded by the GR-135 are notable because the count rates were so low. Count rates were always less than about 1 cps even when the detector was located only 50 cm away from the ^{252}Cf source, which emitted 1.9×10^{5} neutrons per second when the measurements were performed.

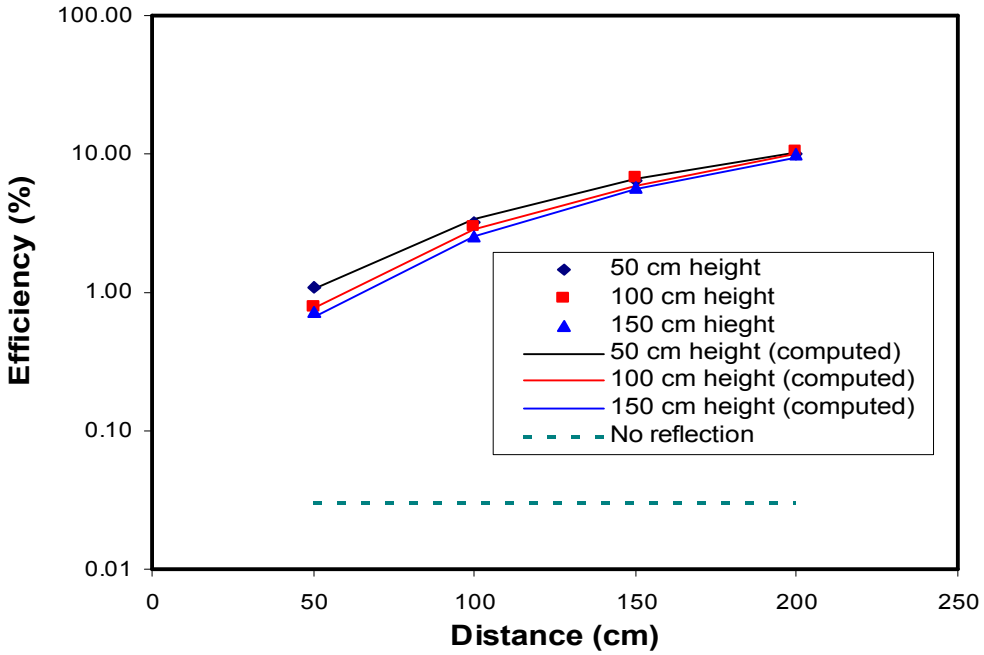

Fig. 2. Neutron detection efficiency of bare ^{3}He tube as a function of distance and height when it is exposed to an unmoderated ^{252}Cf source.

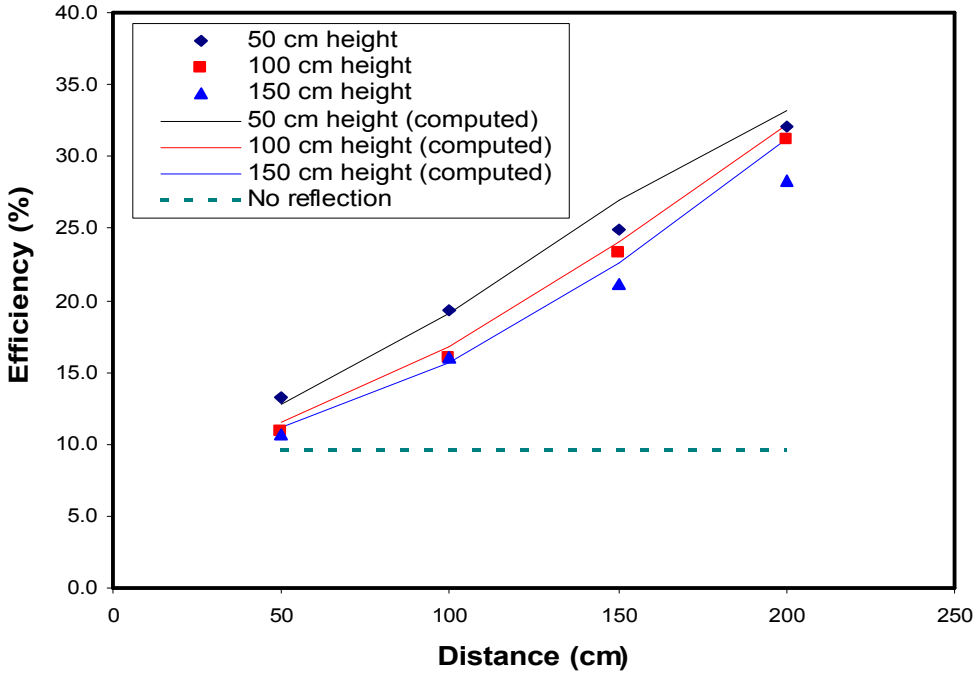

Fig. 3. Neutron detection efficiency of a ^{3}He tube within a 1-inch-thick cylindrical polyethylene moderator when it was exposed to an unmoderated ^{252}Cf source.

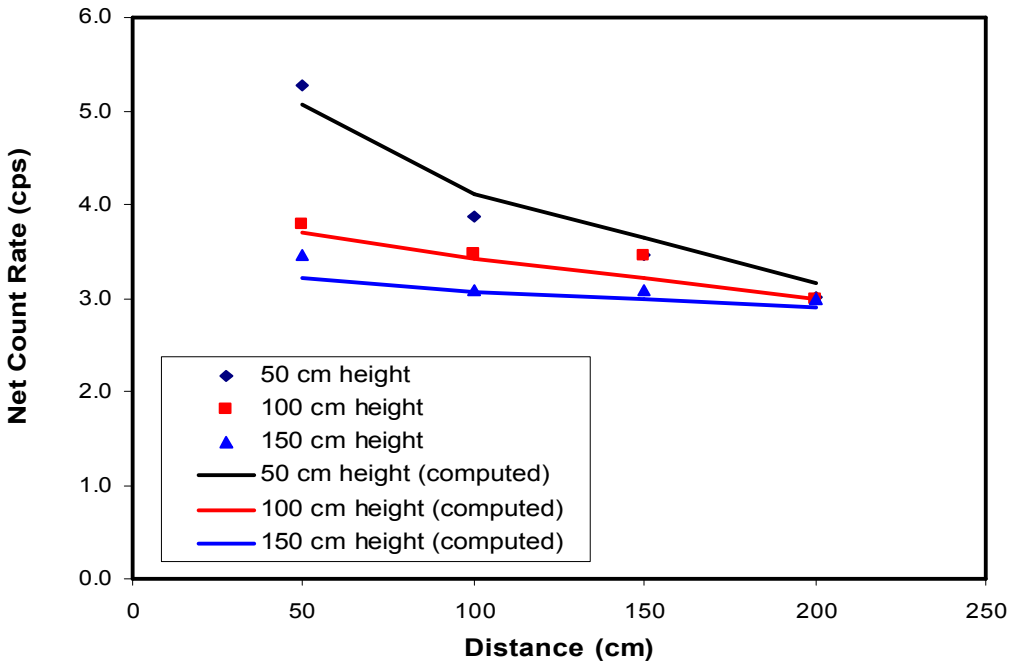

Fig. 4. Neutron count rates as a function of height and distance for a bare ^{3}He tube when it was exposed to a bare ^{252}Cf source.

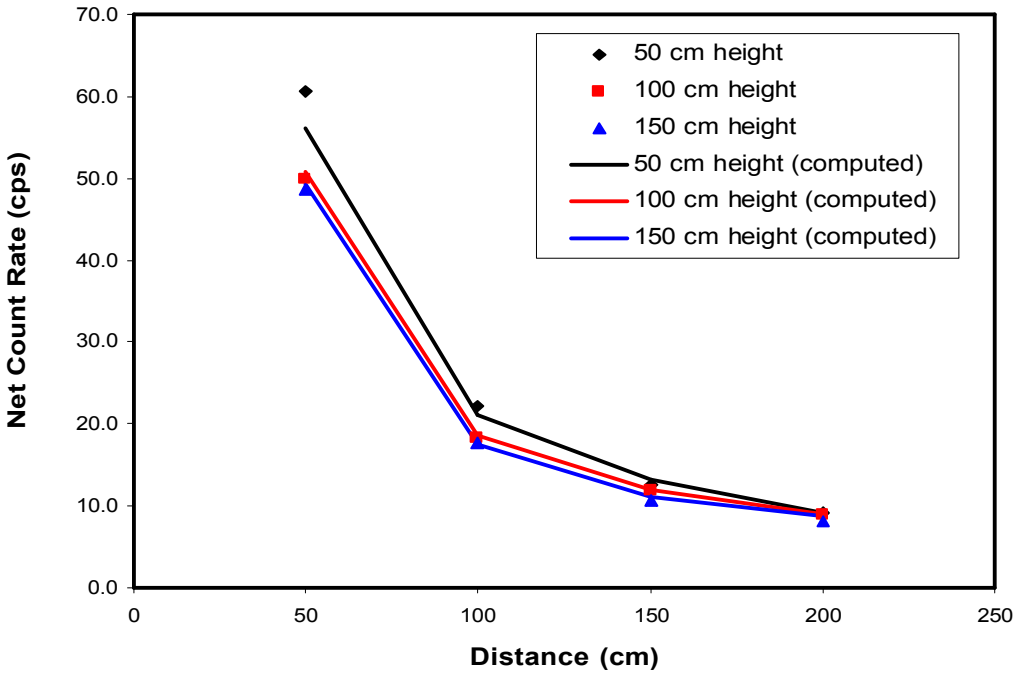

Fig. 5. Neutron count rates as a function of height and distance for a bare ^{3}He tube when it was exposed to a ^{252}Cf source within a 4-cm-thick polyethylene moderator.

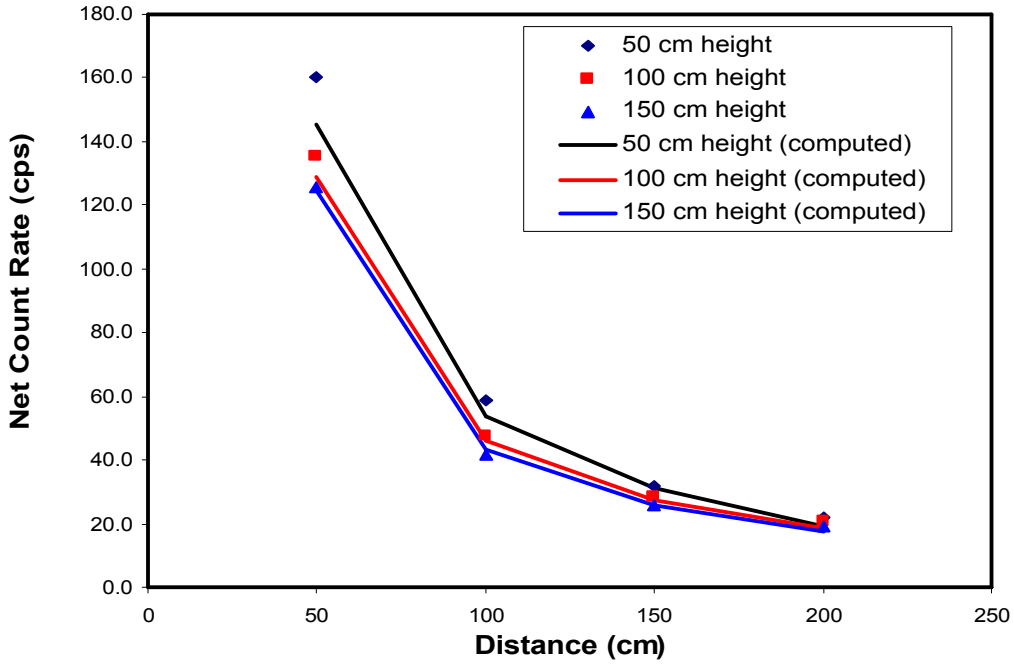

Fig. 6. Neutron count rates as a function of height and distance for a ^{3}He tube within a 1-inch-thick cylindrical polyethylene moderator when it was exposed to a bare ^{252}Cf source.

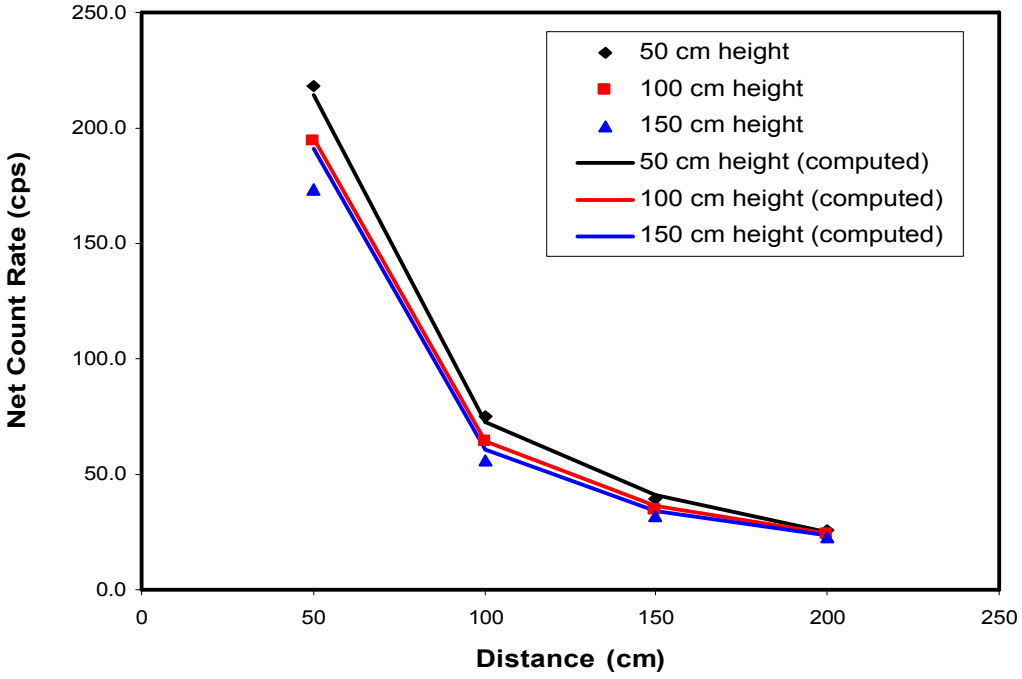

Fig. 7. Neutron count rates as a function of height and distance for a ^{3}He tube within a 1-inch-thick cylindrical polyethylene moderator when it was exposed to a ^{252}Cf source within a 4-cm-thick polyethylene moderator.

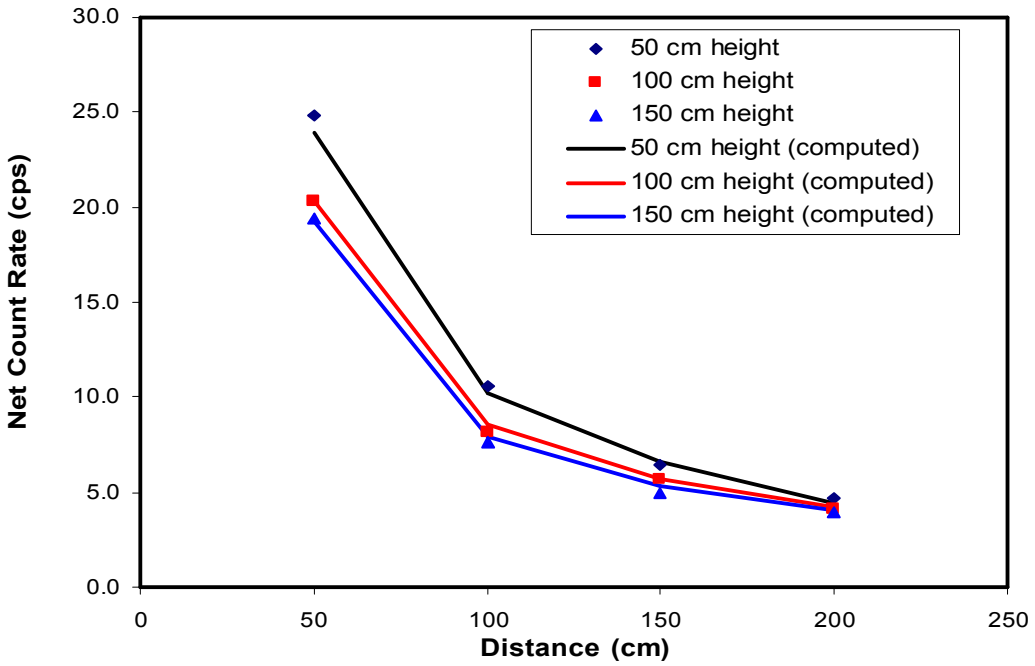

Fig. 8. Neutron count rates as a function of height and distance for an Ortec Detective-EX-100 when it was exposed to a bare ^{252}Cf source.

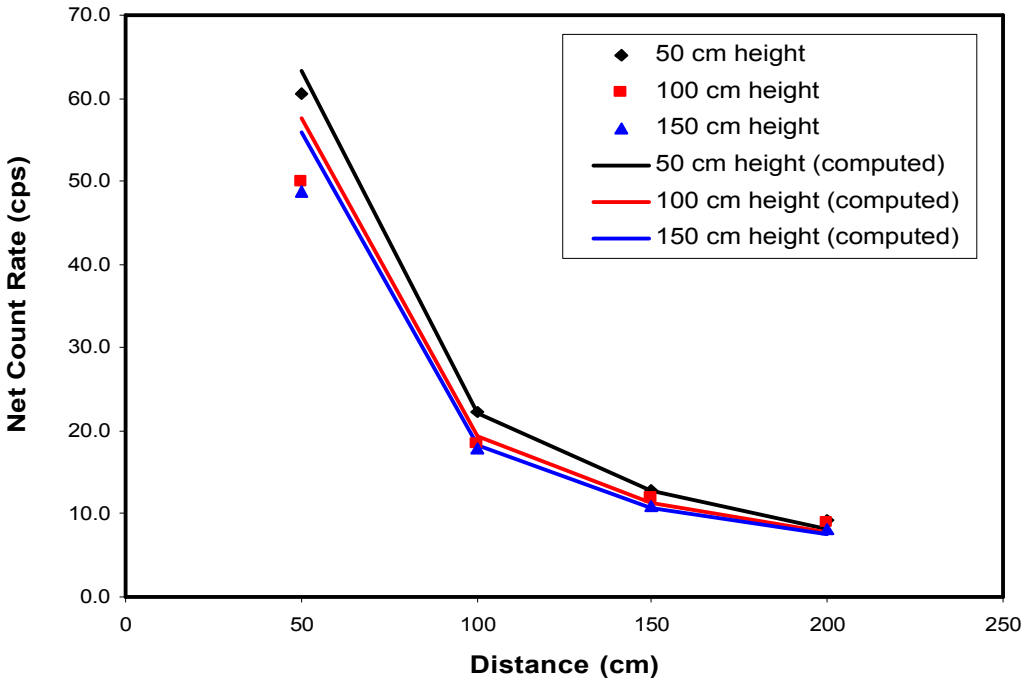

Fig. 9. Neutron count rates as a function of height and distance for an Ortec Detective-EX-100 when it was exposed to a ^{252}Cf source within a 4-cm-thick polyethylene moderator.

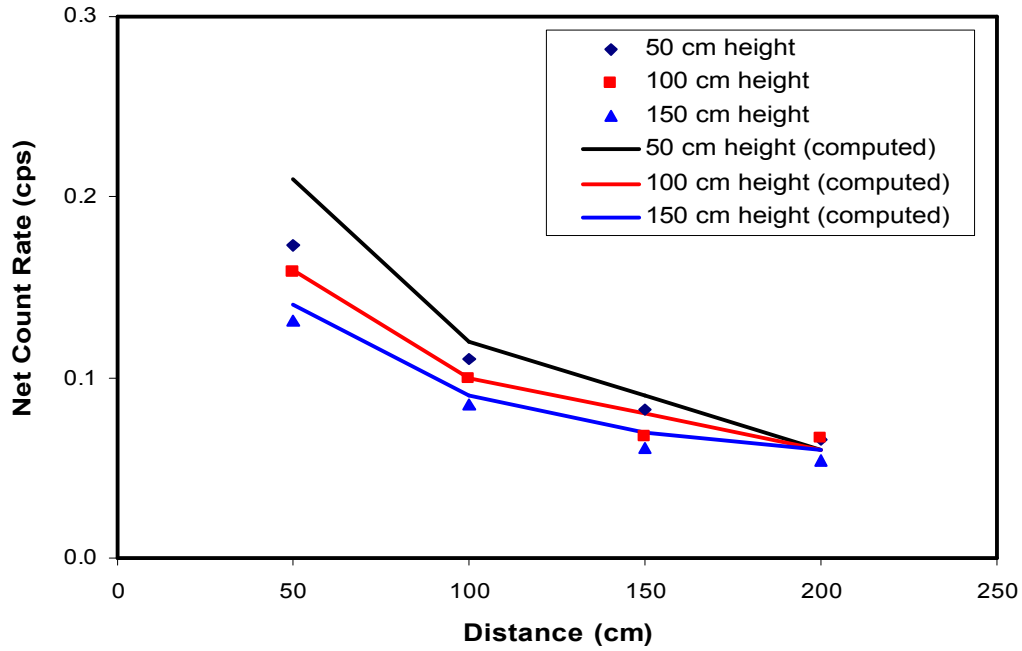

Fig. 10. Neutron count rates as a function of height and distance for a GR-135 when it was exposed to a bare ^{252}Cf source.

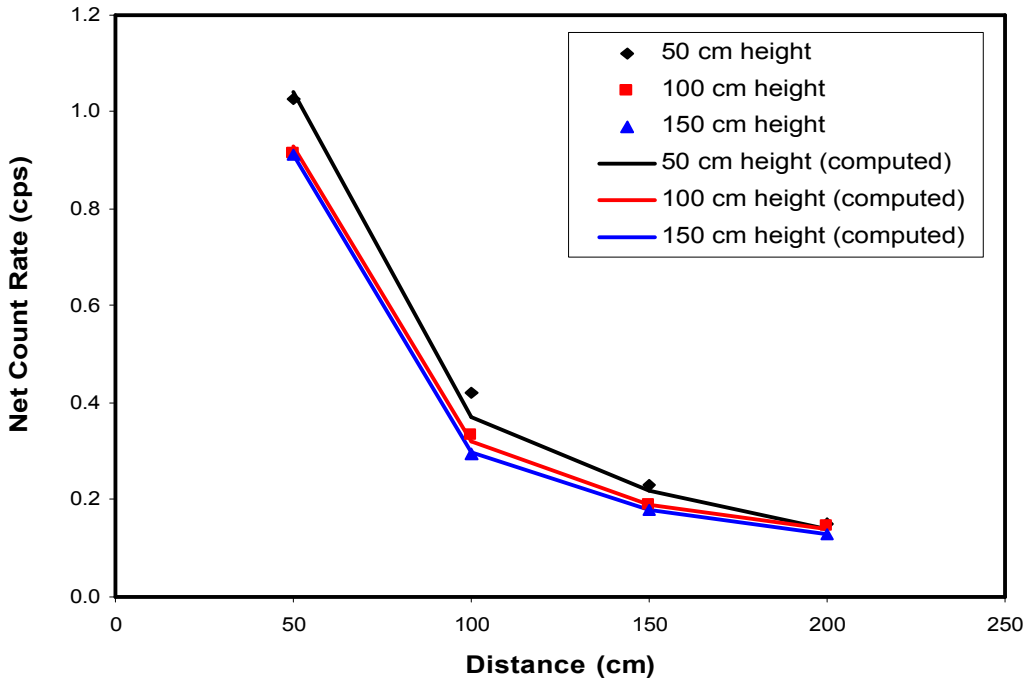

Fig. 11. Neutron count rates as a function of height and distance for a GR-135 when it was exposed to a ^{252}Cf source within a 4-cm-thick polyethylene moderator.

5. GADRAS Interface for Neutron Detectors

The GADRAS Graphic User Interface was modified to accommodate additional features and to display information that may be acquired with neutron detectors. Changes include the following:

- The neutron form is now accessed by striking the top-level menu item *Neutron*, whereas the neutron form was accessed as a sub-menu of *Tools* in previous versions of GADRAS.
- The neutron detector form has been revised to contain four tabs whereas only three tabs were contained in previous versions of GADRAS. The additional tab was added to enable selection among multiple types of neutron detectors that may be contained within a detector folder. Because of the ability to represent one gamma-ray detector plus several types of neutron detector, the detector folders are beginning to assume the significance of project folders rather than only representing one type of detector.
- The revised interface supports multiple types of neutron detectors that can be used in association with a gamma-ray detector. For example, Figure 12 shows the SelectDetector screen that is displayed for a detector folder that contains four types of neutron detectors. The caption for this tab displays the currently selected detector, which can be changed by clicking on one of the entries in the "*Select neutron detector in current folder*" list box. Alternatively, a new neutron detector can be created by clicking on one of the detectors in the "*Clone response from a known type of neutron detector*" list box (see Fig. 12). The user is given the opportunity to rename the neutron detector after cloning the response function parameters.

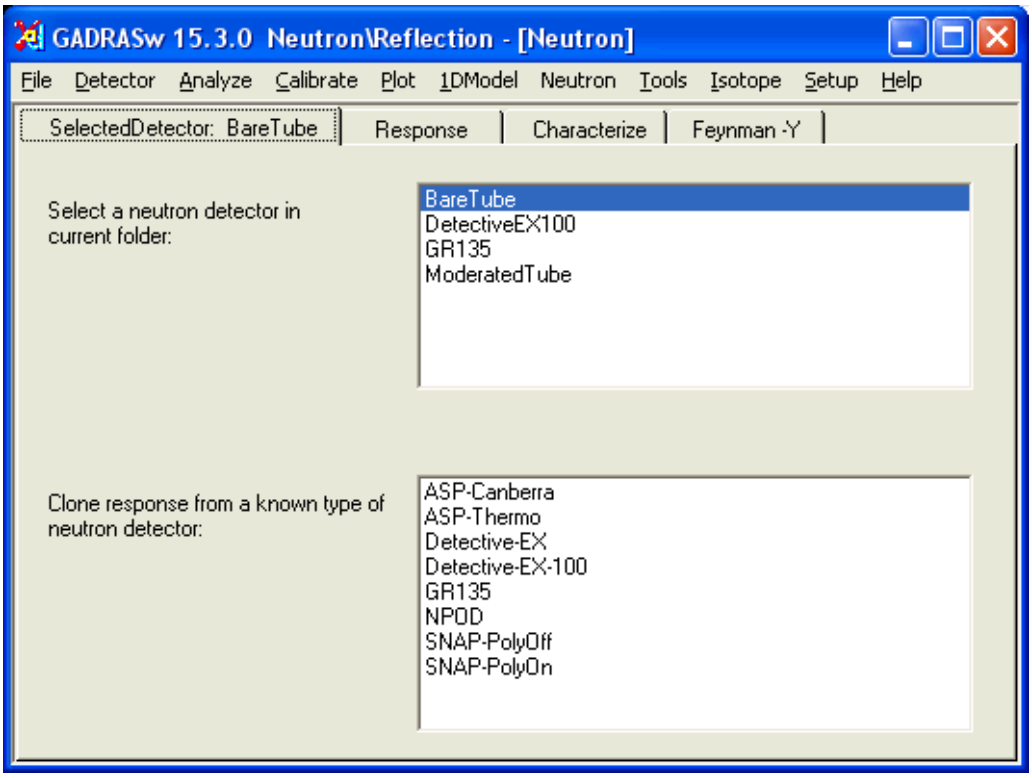

Fig. 12. Screen capture of the form that is displayed while the *SelectDetector* tab is selected under the neutron detector form. Note that the neutron form is accessed by clicking a top-level menu item that is named "Neutron".

Information that is displayed under the *Response* tab has been rearranged to group the fields in a more logical way (see Fig. 13). Users should note that defining the environment, the distance, and the height (displayed in the upper-left quadrant) is essential in order to compute the count rate accurately. These parameters are also contained under the *Characterize* tab, but the environment that pertains to characterization measurements may differ from the environment in which the detector is used during inspections. The parameters that define the two environments are stored separately so that characterization information is not altered when calculations are performed for a different measurements scenario. The efficiency curve that is displayed under the *Response* tab pertains to distance, height, and environment parameters that are defined under this *Response*. These parameters may not be the same as values that are associated measurements of the calibration sources. Typing <Ctrl-C> after clicking on the plot causes the plot to be copied to the clipboard, which enables it to be pasted into documents without necessitating a screen capture of the form.

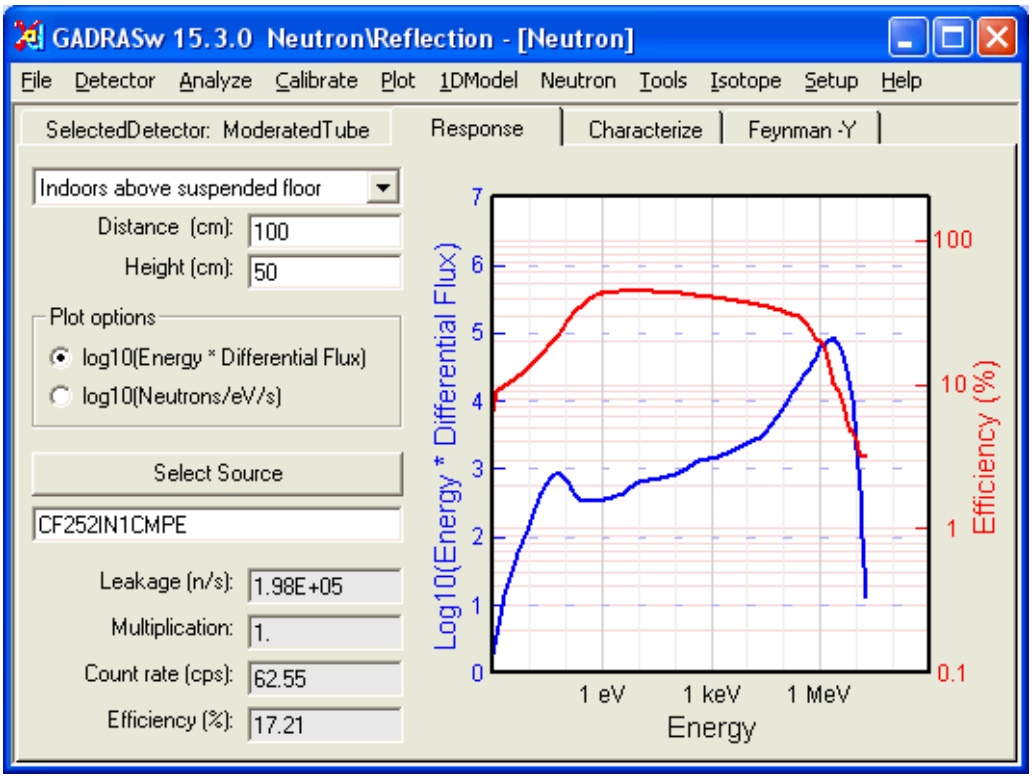

Fig. 13. Screen capture of the form that is displayed while the *Response* tab is selected.

The file-naming conventions and formats for the neutron detector response parameters have also been changed in GADRAS Version 15.3. In previous versions of the application, the neutron detector response parameters were stored in files named "Neutron.dat". These parameters are now stored in files named "Neutron$*DetectorName*.gadras", where the string *DetectorName* varies depending on the name that is specified by the user. A single folder may have several neutron detector parameter files. The file "Neutron.gadras" specifies the last neutron detector that was referenced, which becomes the default detector when GADRAS resumes after a shutdown. Since "dat" is a common file extension, the extension of the neutron parameter file was changed to "gadras" to avoid conflicts with files that are written by other applications. Although GADRAS enables the ability to create new neutron detectors by cloning information from known types of detectors, new detectors can also be created outside of GADRAS by copying the "Neutron$*DetectorName*.gadras" to other detector folders. Data contained in older "Neutron.dat" files are automatically converted to the new file format.

Although the display of characterization information is similar to previous versions of GADRAS, some changes have been made. As shown in Fig. 14, the characterization information now includes the description of the environment, the distance, and the height in the upper-left corner of the form, which is similar to the location for equivalent parameters on the *Response* tab. As with previous versions of GADRAS, parameters that are selected as adjustable are highlighted with a cyan background, and these settings can be changed by clicking on the parameter label. One thing that you will note is that the estimated background count rate is presented on the first line of the "Computed (cps)" text box (lower-right corner). The background count rate is computed based on the location at which the detector was characterized. A command button labeled "Location?" is presented until this information is entered. The location information can be changed subsequently by clicking on the "Computed (cps)" text box. The accuracy of the background neutron count rate is not as accurate as desired, and future work will focus on improving the radiation background model.

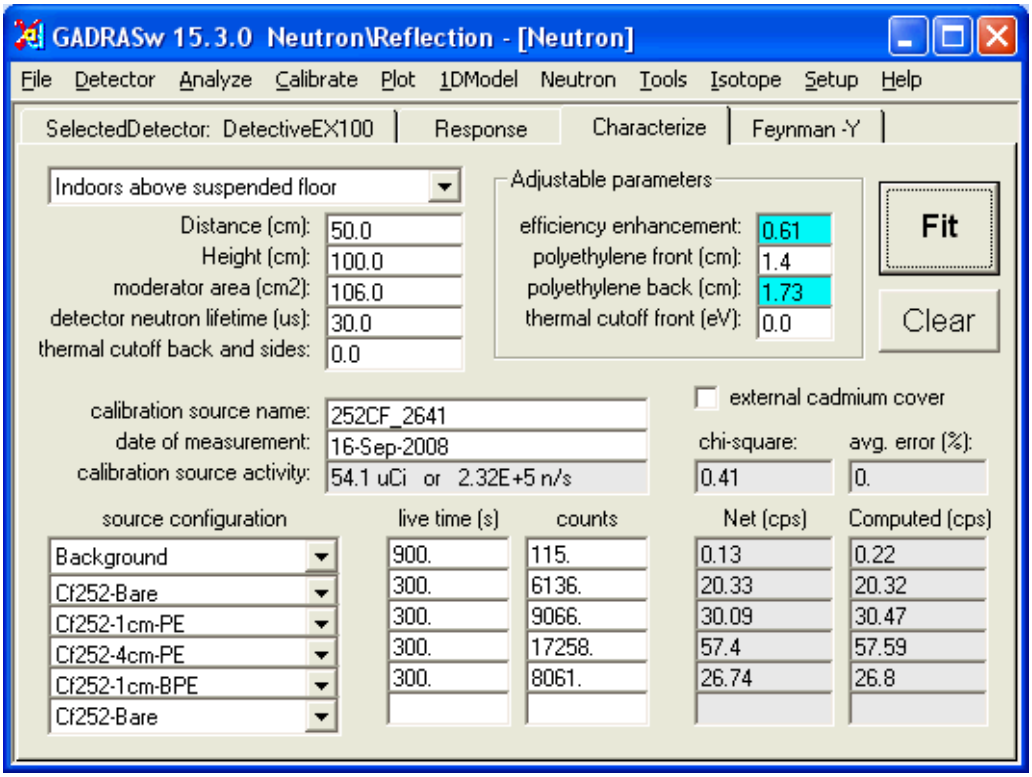

Fig. 14. Screen capture of the form that is displayed while the *Characterize* tab is selected.

The fourth tab on the "Neutron" form is accessed compare computed and measured neutron-time-correlation metrics. The metric that is presented in this plot is the Feynman-Y distribution [5]. The relationship between the Feynman-Y value and the gate width can be displayed in a linear plot, as shown in Fig. 15, or a log-log plot can be presented. Dragging the cursor across a selected region causes the plot to be redrawn for the selected region. Starting or finishing the drag operation outside of the plot area causes the plot to revert to the full range. Striking <Ctrl-C> copies the plot to the Windows clipboard.

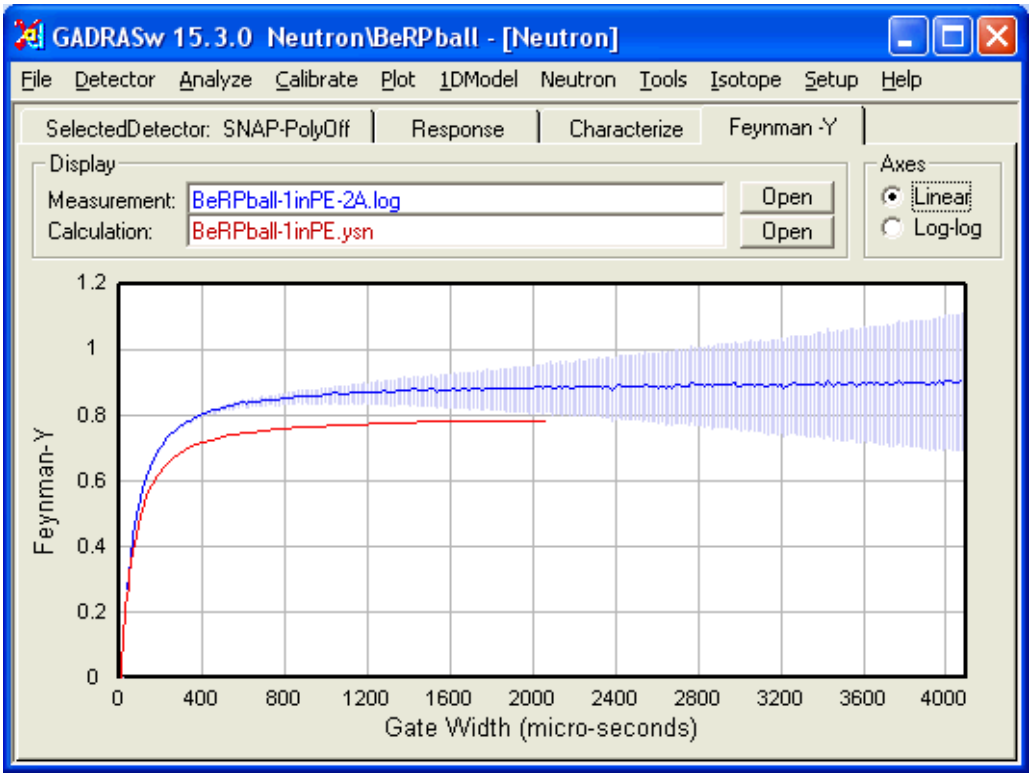

Fig. 15. Screen capture of the form that is displayed while the *Feynman-Y* tab is selected.

6. Future Work

Development of the revised neutron detector response model is essentially complete. However, a few aspects of the response model need to be improved or validated, as itemized below:

- Computed count rates were compared with measurements for numerous detectors, and the energy distributions of neutron flux calculations based on our implementation of the PARTISN code were also compared with MCNP. The agreement is generally good, but discrepancies are observed in a few cases. We have found that the computed leakages of neutrons in the thermal region are high by as much as 30% for ^{252}Cf with only a small amount of moderator. Thermal neutrons are only important for neutron detectors with little moderator, and the effects are noticeable for the bare ^{3}He tube that was discussed in this report. However, this discrepancy is relatively unimportant for most neutron detectors, even those containing only a small amount of moderator. Nevertheless, an effort will be made to correct these deviations with future software upgrades.
- Measurements that were described in this report were all recorded in one laboratory environment. Although calculations were also compared with measurements for neutron detectors that were measured previously, systematic measurements over a range of distances and heights are not available. Future work may include similar measurements for other environments.
- Computed background neutron count rates do not always agree with measurements. Additional measurements and calculations will be performed to address this deficiency.

Acknowledgement

This work was funded by the Department of Homeland Security (DHS) Domestic Nuclear Detection Office (DNDO).

References

[1] Dean J. Mitchell, Thomas W. Laub, and Keith W. Marlow, *Semi-Empirical Response Function for Neutron Detectors*, Sandia National Laboratories Report SAND93-2570 (October 1993).

[2] X-5 Monte Carlo Team, *MCNP - a general purpose Monte Carlo N-particle Transport code, version 5*, Technical report LA-UR-03-1987, Los Alamos National Laboratory, Los Alamos, NM, 87545 (October 2003).

[3] Lee T. Harding, John K. Mattingly, and Dean J. Mitchell, *Modernized Neutron Efficiency Calculations for GADRAS*, Sandia National Laboratories Report SAND2008-6073 (September 2008).

[4] Eric S. Varley and John Mattingly, "Rapid Feynman-Y Synthesis: Kynea3 Cross-Section Library Development," *Trans. Am. Nucl. Soc*. 98, 2008, pp. 575-576.

Sandia is a multiprogram laboratory operated by Sandia Corporation, a Lockheed Martin Company, for the United States Department of Energy's National Nuclear Security Administration under Contract DE-AC04-94AL85000.